



**Please cite the Published Version**

Gao, Z, Liu, H, Kulczyk-Malecka, J , Liu, C, Hu, D, Kelly, P  and Xiao, P (2023) Substrate controlled degradation rate of protective SiAlN coating via mitigating interfacial reaction. Corrosion Science, 213. p. 111006. ISSN 0010-938X

**DOI:** <https://doi.org/10.1016/j.corsci.2023.111006>

**Publisher:** Elsevier

**Version:** Accepted Version

**Downloaded from:** <https://e-space.mmu.ac.uk/631444/>

**Usage rights:**  [Creative Commons: Attribution-Noncommercial-No Derivative Works 4.0](https://creativecommons.org/licenses/by-nc-nd/4.0/)

**Additional Information:** This is an Author Accepted Manuscript of an article published in Corrosion Science, published by and copyright Elsevier.

**Data Access Statement:** Data will be made available on request.

**Enquiries:**

If you have questions about this document, contact [openresearch@mmu.ac.uk](mailto:openresearch@mmu.ac.uk). Please include the URL of the record in e-space. If you believe that your, or a third party's rights have been compromised through this document please see our Take Down policy (available from <https://www.mmu.ac.uk/library/using-the-library/policies-and-guidelines>)

# Substrate controlled degradation rate of protective SiAlN coating via mitigating interfacial reaction

Zhaohe Gao<sup>a,b\*</sup>, Han Liu<sup>a</sup>, Justyna Kulczyk-Malecka<sup>c</sup>, Conghui Liu<sup>a</sup>, Dongchen Hu<sup>a</sup>, Peter Kelly<sup>c</sup> and Ping

Xiao<sup>a\*</sup>

<sup>a</sup>Henry Royce Institute, Department of Materials, University of Manchester, Manchester, M13 9PL, UK

<sup>b</sup>School of Metallurgy & Materials, University of Birmingham, Birmingham, B15 2TT, UK

<sup>c</sup>Surface Engineering Group, Manchester Metropolitan University, Manchester, M1 5GD, UK

## Abstract

The degradation rates of protective SiAlN coatings (0.9  $\mu\text{m}$  thick) on pure Ti, Ti6Al4V, and Timetal 834 alloys in air at 800°C were investigated and compared. The SiAlN coating on pure Ti was depleted and then formed a thin oxide scale after exposure of 50 h, whereas a 0.6  $\mu\text{m}$  thick remnant SiAlN coating without any signs of oxidation was observed on Timetal 834. Interfacial reactions between SiAlN coatings and different substrates caused depletion of SiAlN, thereby determining the degradation rates of SiAlN coatings. The non-reactive alloying elements Sn and Al in Timetal 834 alloy could retard such interfacial reactions, thereby impeding coating degradation.

**Keywords:** Protective coating; Interfacial depletion; Oxidation; Degradation; Ti alloys

## 1. Introduction

Ti alloys are widely applied in gas turbine aeroengines and hybrid-electric airplanes due to their low density and high specific strength [1-5]. In fuel-efficient innovations for aeroengines or hybrid-electric airplanes, Ti alloys have found applications in components exposed to relatively high temperature and chemically aggressive demanding environments, e.g. as a fan blade (Ti6Al4V), compressor (Ti6246 or Timetal 834), or turbine blade (low pressure, TiAl alloys) [6-8]. However, Ti alloys have inadequate oxidation resistance at high temperatures, which restricts their applications for fuel-efficient innovations [4, 9]. Therefore, the application of Ti alloys relies on coatings technologies allowing for improved oxidation resistance of the Ti alloys in such harsh environments [4]. Thermally stable and amorphous SiAlN ( $\text{Si}_3\text{N}_4/\text{AlN}$ ,  $\text{Si}_3\text{N}_4$  is the matrix) coatings with Mo interlayers on Ti substrates have displayed excellent oxidation resistance in an air environment at high temperatures in our previous work [10]. The SiAlN coating exhibited good thermal stability at high temperature as the outermost

protective layer in this coating design, and the Mo interlayer provided good interfacial performance due to its diffusion into the underlying Ti substrate. However, the one-micrometer thick SiAlN layer is continuously consumed by the underlying Ti upon thermal exposure due to chemical incompatibility. Increasing the thickness of the as-deposited SiAlN layer seems to be the most obvious solution to this, but, the inherently slow deposition rate of SiAlN (e.g.  $\sim 1 \mu\text{m}$  thickness of SiAlN per two hours) by magnetron sputtering, in comparison with the thermal spray technique, and the fact that relatively thick coatings often cause high residual stresses within the coating, restricts the maximum practical thickness of the SiAlN coating in this design [11, 12]. Therefore, the desirable approach would be to mitigate the interfacial reaction between Ti and SiAlN, and thereby the depletion of SiAlN, by introducing non-reactive alloying elements into the Ti substrate.

In this study, we deposited a series of identical  $0.9 \mu\text{m}$  thick SiAlN coatings with a Mo interlayer on pure Ti, Ti6Al4V, and Timetal 834 alloys substrates by magnetron sputtering. After identical thermal exposure, the SiAlN coatings on the different substrates degrade at different rates due to different interfacial reactions. And the effects of the alloying elements, Al and V in Ti6Al4V, Al, Sn, Zr, and Nb in Timetal 834 on the interfacial reactions have been examined.

## 2. Experiments and methods

The SiAlN coatings with Mo interlayers were deposited on one side of commercially pure Ti (>99.6 wt % Ti), Ti6Al4V (Ti-6Al-4V, wt %) alloy, and Timetal 834 (Ti-5.8Al-4Sn-3.5Zr-0.7Nb-0.5Mo-0.35Si-0.06C, wt %) alloy substrates using a UDP 350 magnetron sputtering system (Teer Coatings Ltd), equipped with 3 off  $300 \text{ mm} \times 100 \text{ mm}$  unbalanced magnetrons vertically installed through the chamber walls. Before deposition, the Ti and Ti alloy substrates were ground, polished, and ultrasonically cleaned. The polished coupons were then mounted on a centrally rotating unheated substrate holder inside the sputtering chamber. The substrates were sputter cleaned at a DC bias of -600 V for 15 minutes. After cleaning, the Mo deposition was carried out in an Ar only environment with the Mo target was powered by a pulsed DC power supply at a power of 500 W and 100 KHz pulse frequency, 60% duty. Following that, the deposition of SiAlN was carried out in an Ar and  $\text{N}_2$  atmosphere, and the Si and Al targets were powered at 700 W and 300 W (100 kHz at 60% duty), respectively. During all deposition stages, a bias of -30 V was applied to the substrate holder and the substrate holder was rotated at a speed of 5 rpm, full details were reported in our previous work [10].

The SiAlN/Mo coated Ti, Ti6Al4V, and Timetal 834 coupons were tested by thermal cycling at  $800^\circ\text{C}$  for 5 h in atmospheric pressure air in a programme controlled CM<sup>TM</sup> furnace with a heating rate of  $100^\circ\text{C} / \text{minute}$  and followed by forced air cooling for 10 minutes (sample stage out of the heating

zone), then returned for the next cycle. The testing conditions for the identical coatings on pure Ti, Ti6Al4V and Timetal 834 was consistent as three groups of samples were placed together into the hot zone of the furnace each time. The testing duration (5 h for each cycle) was adjudged to start when the temperature reached 800°C. The cross-sectional observation of the thermal cycled SiAlN/Mo coated Ti or Ti alloys was carried out by scanning electron microscopy (SEM). To investigate the microstructure and composition of the as-deposited and thermal cycled samples, thin lamellae were prepared by FIB via a lift-out technique and then studied by transmission electron microscopy (TEM, FEI, Talos F200) fitted with a Super - X- EDS system.

### 3. Results and Discussion

Fig.1 a shows a cross-sectional SEM micrograph of the as-deposited SiAlN (~930 nm thick) coating with a Mo interlayer on a pure Ti substrate. The SiAlN coating shows a smooth, dense, and homogeneous microstructure without any signs of defects, as shown in Fig.1 b – b2. The Mo interlayer provides a bonding role between the nitride coating and the substrate. Identical SiAlN coatings with Mo interlayers were also deposited on Ti6Al4V and Timetal 834 alloys. The SiAlN coatings were amorphous and consisted of amorphous Si<sub>3</sub>N<sub>4</sub> and AlN phases, where amorphous AlN phases were dispersed in the Si<sub>3</sub>N<sub>4</sub> matrix, as reported in our previous work [10].

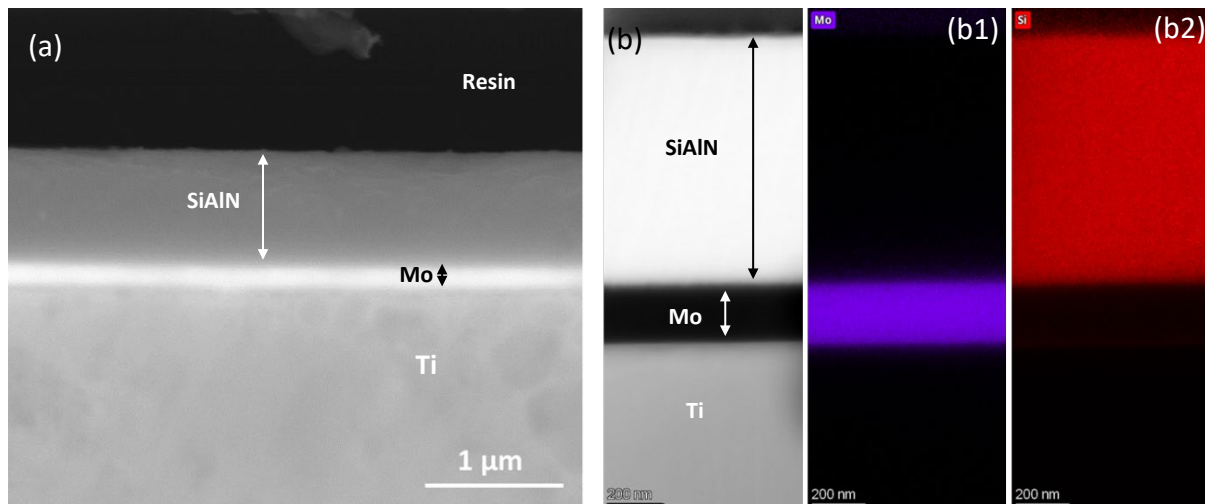


Fig. 1 Cross-sectional microstructural and compositional analysis of as-deposited SiAlN/Mo coating on Ti. (a) SEM micrograph, (b), (b1) and (b2) STEM micrograph and corresponding EDS maps.

The identical SiAlN/Mo coatings deposited on Ti, Ti6Al4V, and Timetal 834 substrates were also thermally cycled at 800°C in air to compare the effects of different substrate materials on the coatings' degradation. Figs. 2 a, b and c show cross-sectional SEM images of SiAlN/Mo coatings on Ti, Ti6Al4V, and Timetal 834 alloys, respectively, after oxidation at 800°C in air for 20 h (4 cycles). All the coated

samples provide good oxidation protection in comparison with bare Ti or its alloys. However, the SiAlN coatings on different substrates degrade at different rates. The SiAlN coating on Ti has been fully depleted and a thin oxide scale (mainly consisting of  $\text{TiO}_2$ ,  $\sim 0.9 \mu\text{m}$  thick) has formed on top, while a  $\sim 250 \text{ nm}$  thick leftover SiAlN layer was observed on Ti6Al4V and a  $\sim 850 \text{ nm}$  thick remnant SiAlN layer was observed on Timetal 834, as shown in Fig. 2. The SiAlN coated Ti surface starts to oxidise once the remnant SiAlN coating is close to being depleted or fully depleted and the oxide scale mainly consists of  $\text{TiO}_2$ , confirmed and illustrated in Fig. S1 in Supplementary Material. Extending the thermal cycling duration from 20 h to 50 h (10 cycles), showed that the oxide scale on the SiAlN/Mo coated pure Ti thickens to  $\sim 5.0 \mu\text{m}$ , the SiAlN coating on Ti6Al4V is close to depletion, while the SiAlN coating on Timetal 834 remains considerably thicker ( $\sim 0.6 \mu\text{m}$ ), as shown in Fig.2 a1 to c1, respectively. It is evident that different Ti-based substrates have a significant impact on the degradation of the SiAlN coatings. Noticeably, interdiffusion and the interfacial reaction between SiAlN/Mo and the underlying Ti or Ti alloys have been observed in Fig. 2, and such interfacial diffusion/reaction is the key element in determining the degradation rate of SiAlN coatings.

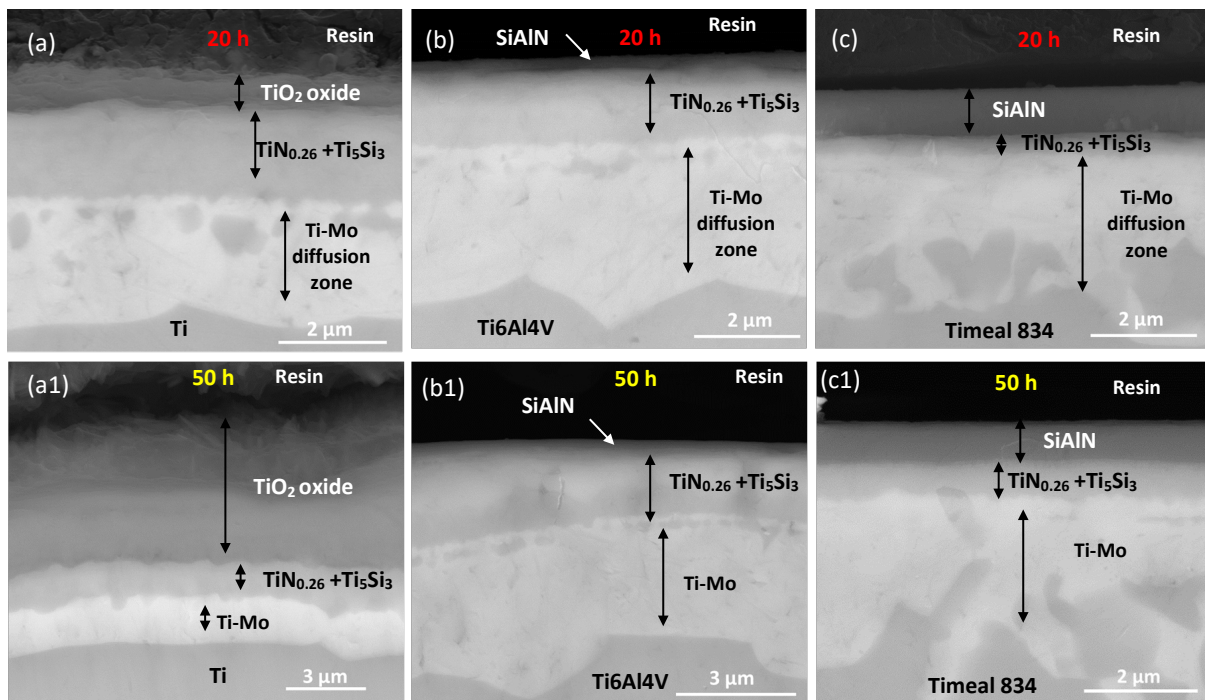


Fig.2 Cross-sectional SEM image of SiAlN/Mo coating on different Ti alloys after oxidation at  $800^\circ\text{C}$  in air for 20 h (4 cycles) and 50 h (10 cycles). (a) and (a1) Pure Ti, (b) and (b1) Ti6Al4V alloy, (c) and (c1) Timetal 834.

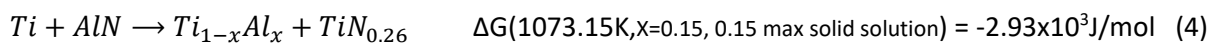
In order to examine the interfacial diffusion and reaction in finer detail, thin lamellae of cross-sections of the SiAlN/Mo coated Ti6Al4V and Timetal 834 alloys after oxidation at  $800^\circ\text{C}$  for 20 h (4 cycles) were prepared by FIB and studied by TEM. Fig.3 shows the cross-sectional micrographs and EDS maps of

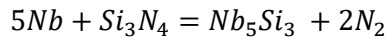
the SiAlN/Mo coated Ti6Al4V alloy after oxidation at 800°C for 20 h (4 cycles). No obvious oxide scale forms on the remnant SiAlN coating and the SiAlN coating has been depleted to ~ 250 nm thick, confirmed by the HAADF micrograph and EDS maps in Fig.3 a and b. During thermal exposure, the Ti-Mo interdiffusion zone can form rapidly due to the relatively high diffusivity of Mo in Ti ( $2.38 \times 10^{-14}$  cm<sup>2</sup>/sec, at 800°C) and the complete solubility between Mo and Ti [13, 14]. Simultaneously, Ti from the Ti-Mo zone or the Ti6Al4V (wt %) alloy can react with Si<sub>3</sub>N<sub>4</sub> and the AlN (matrix Si<sub>3</sub>N<sub>4</sub> with minor amounts of the AlN phase; the below reactions mainly focus on Si<sub>3</sub>N<sub>4</sub>), mainly forming TiN<sub>0.26</sub> and Ti<sub>5</sub>Si<sub>3</sub>, as shown in equation 1 below, also marked in Fig.3 a and well reported in our previous work [10]. The 4 wt% (3.6 at%) V as a solid solution in Ti alloys can also react with Si<sub>3</sub>N<sub>4</sub> based on the Gibbs reaction energy calculated by Thermocalc, as shown in equation 2. Also, the 6 wt% (10.19 at%) Al as a solid solution in Ti6Al4V has been reported to react with Si<sub>3</sub>N<sub>4</sub>, and the reaction products are AlN and Si, as described in equation 3 [15, 16]. However, both AlN and Si can further react with Ti forming TiN<sub>0.26</sub> and Ti(Al) (Al is distributed in the underlying Ti as a solid solution) [10], and Ti<sub>5</sub>Si<sub>3</sub>, as shown in equations 4 and 5, respectively. Noticeably, there is an Al rich layer underneath the interfacial reaction zone (Fig.3 a and b, Al map) and thereby it can be expected that the Al has a retarding effect on the interfacial reaction between SiAlN and the underlying substrate in comparison with Ti, more details are given below.

For the Timetal 834 case, no obvious oxide scale forms on the remnant SiAlN coating after 20 h (4 cycles) oxidation, and the remaining SiAlN coating is ~ 850 nm thick, confirmed in Fig.4. The SiAlN coating on Timetal 834 depletes more slowly than that on Ti6Al4V alloy after an identical thermal exposure. The Ti and 5.8 wt% (10.26 at%) Al in Timetal 834 can react with Si<sub>3</sub>N<sub>4</sub> (SiAlN), as discussed above and described in equations 1, 3, 4 and 5. Also, the alloying elements of 3.5 wt% (1.83 at%) Zr [17] and 0.7 wt% (0.35 at%) Nb in Timetal 834 can react with Si<sub>3</sub>N<sub>4</sub>, as shown in equations 6 and 7, respectively. Noticeably, the 4 wt% (1.6 at%) Sn cannot react with Si<sub>3</sub>N<sub>4</sub> due to the lack of proper corresponding reaction products [18, 19]. Sn has also been observed to form a Sn rich layer underneath the interfacial reaction zone, as shown in Fig. 5. Thus, it can be expected that Sn has a sluggish effect on the interfacial reaction between SiAlN and the underlying Timetal 834 substrate.

The amorphous SiMeN (Me=Al, Zr, Ti, Cr, etc.) coatings display good intrinsic thermal stability due to their high activation energy and extremely low parabolic rate constant of oxidation [11, 17]. However, the degradation of SiMeN is determined by the interfacial diffusion/reaction with the underlying substrate as the interdiffusion/inter-reaction could alter the microstructure and chemical composition of the top amorphous SiMeN coating, or cause the depletion of the remnant SiMeN coating [11, 17,20]. The degradation of SiAlN/Mo on Ti or Ti alloys is controlled by its depletion, confirmed in Fig.S1 and

illustrated by Scenario III in Fig.S2 (Supplementary Material), respectively. The SiAlN coated Ti or Ti alloys surface starts to oxidise once the remnant SiAlN coating is close to being depleted or fully depleted. The above results have shown that the depletion rates of SiAlN coatings induced by interfacial reaction with different substrates (Ti, Ti6Al4V, Timetal 834) are different, thereby playing a significant role in the degradation rate of the SiAlN coating. Thermodynamically, with the exception of Sn, the elements as a solid solution present in Ti or Ti alloys, i.e., Ti, Al, V, Zr, and Nb, can react with the Si<sub>3</sub>N<sub>4</sub> from the SiAlN coating, continuously causing the interfacial depletion of the remnant SiAlN. All the potential reactions between alloying elements and SiAlN have been calculated by Thermocalc (in this work a list of only some of the reaction equations is provided), and it is difficult to investigate each reaction rate considering the complexity of such a large number of reactions. And the interlayer Mo is expected to have negligible effect (or identical effect for the three substrates tested here) on the depletion of SiAlN, as Mo rapidly diffuses away from the interface into the underlying substrates and Mo cannot react with Si<sub>3</sub>N<sub>4</sub>, as confirmed by Fig.2 to 4 and Thermocalc. Among the interfacial reactions, the reaction products between Al and Si<sub>3</sub>N<sub>4</sub> can further react with the abundant Ti, described in equations 3, 4, and 5, and thereby the most thermodynamic favourable reaction are reactions 4 and 5. It can be expected that the Al elements from Ti6Al4V or Timetal 834 would play a retarding effect on the interfacial reaction with Si<sub>3</sub>N<sub>4</sub> in comparison with Ti elements from the Ti alloys. Moreover, the activities of Ti in pure Ti, Ti6Al4V and Timetal 834 alloys were calculated, and Timetal 834 has the lowest value, followed by Ti6Al4V and pure Ti, as shown in Fig.6. Thus, the SiAlN/Mo coating on pure Ti has a relatively faster interfacial reaction rate, compared to that on Ti6Al4V, causing the complete depletion of the SiAlN coating and resulting in the formation of oxide scale. The non-reactive 4 wt% (1.6 at%) Sn along with sluggish 5.8 wt% (10.26 at%) Al in Timetal 834 alloy and the lowest Ti activity enable Timetal 834 alloy to have the slowest interfacial reaction between SiAlN and the underlying substrates among pure Ti, Ti6Al4V, and Timetal 834 alloys.





$$\Delta G(1073.15K) = -1.03 \times 10^5 \text{ J/mol} \quad (7)$$

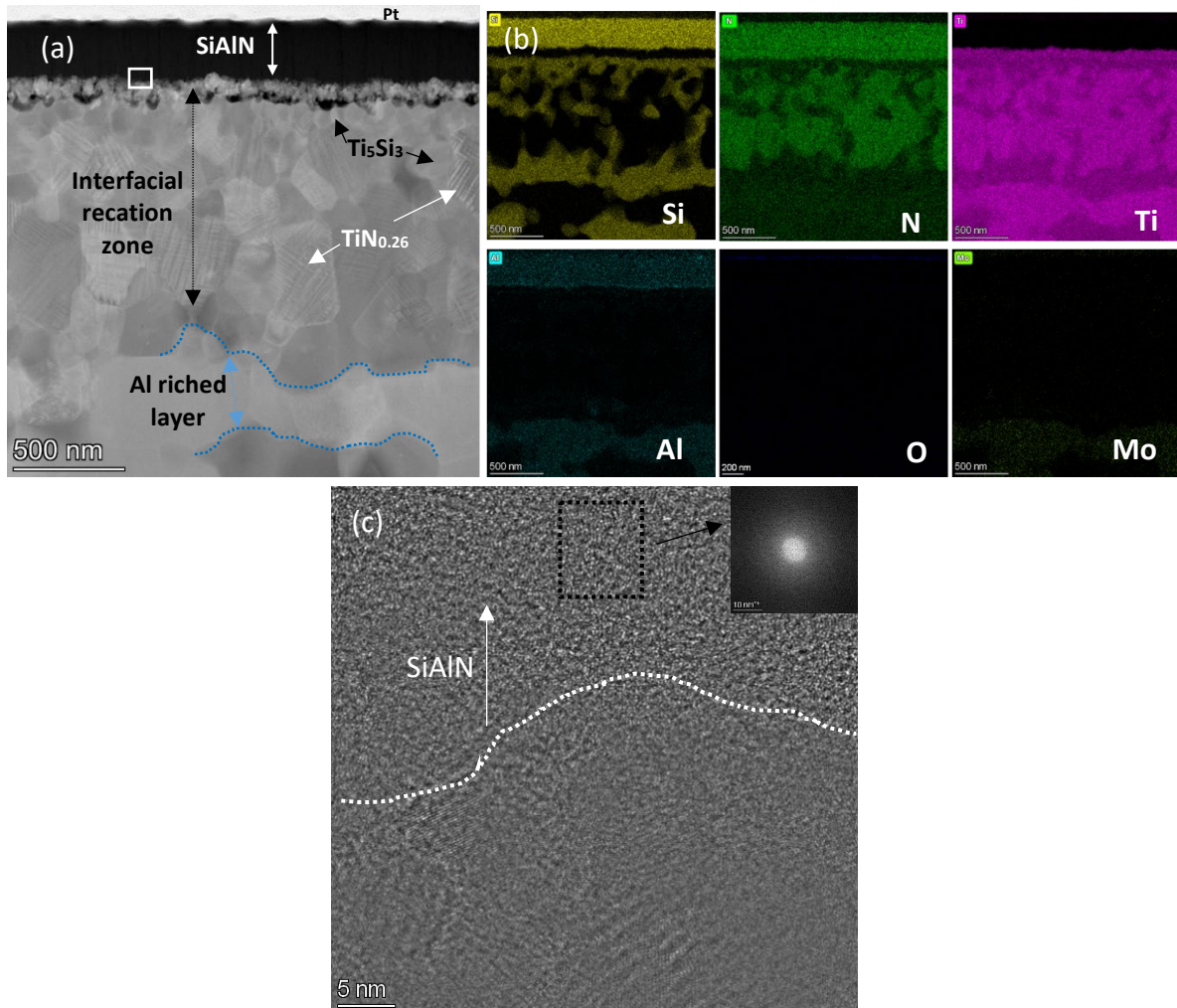


Fig.3 Cross-sectional micrographs and EDS maps of SiAlN/Mo coating on Ti6Al4V alloy after oxidation at 800°C for 20 h (4 cycles). (a) and (b) HAADF micrography and corresponding EDS maps; (c) HRTEM image, acquired from the rectangle box in (a), the corresponding FFT showing the amorphous status of the remnant SiAlN coating.



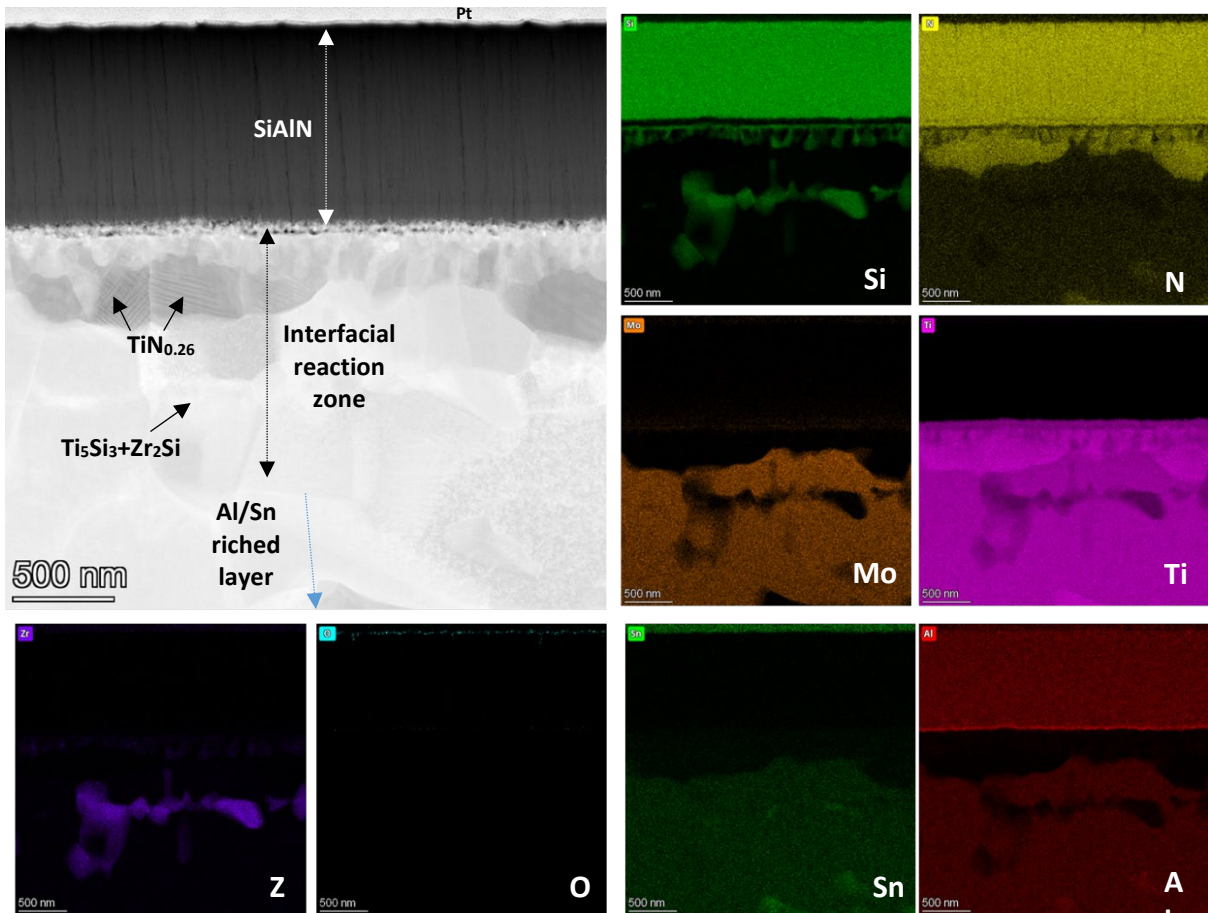


Fig. 4 Cross-sectional HAADF micrograph and EDS maps of SiAlN/Mo coating on Timetal 834 alloy after oxidation at 800°C for 20 h (4 cycles).

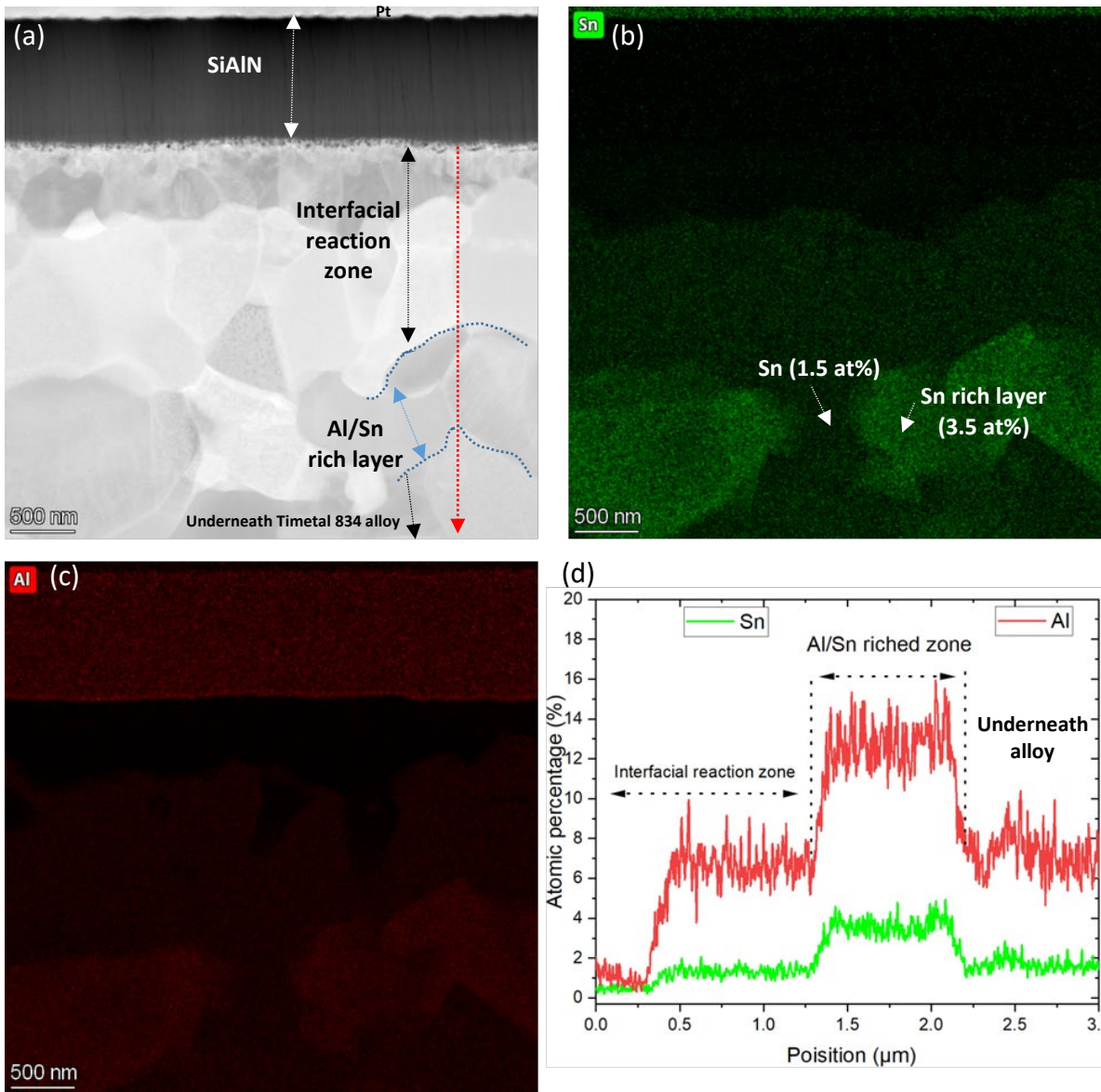


Fig.5 Cross-sectional HAADF micrograph and compositional analysis of SiAlN/Mo coating on Timetal 834 alloy after oxidation at 800°C for 20 h (4 cycles). (a), (b) and (c) HAADF micrograph and corresponding EDS maps of Sn and Al; (d) EDS line analysis of Sn and Al, acquired from the line in (a).

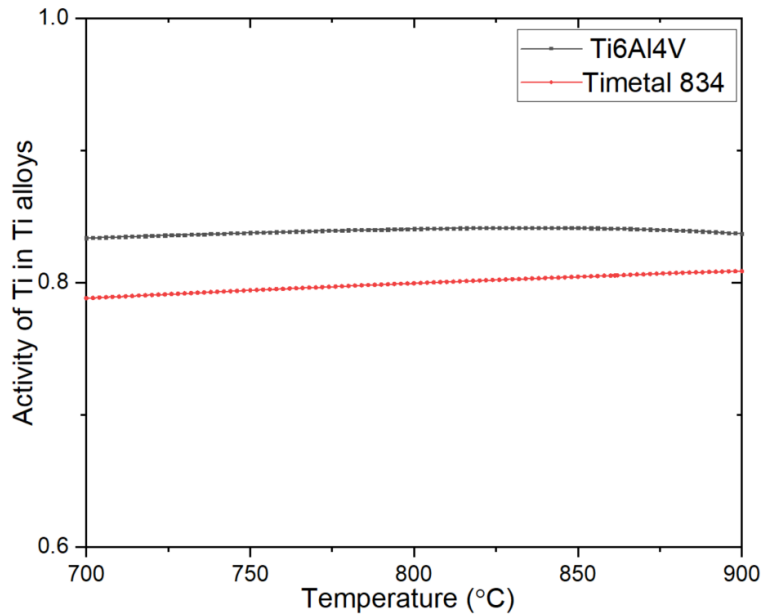


Fig.6 Activity of Ti in Ti6Al4V and Timetal 834 as function of temperature; Ti in pure Ti regarding as 1.

#### 4. Conclusion

In conclusion, amorphous 0.9  $\mu\text{m}$  thick SiAlN coatings with Mo interlayers have been deposited on pure Ti, Ti6Al4V, and Timetal 834 alloys by magnetron sputtering. The degradation rates of the protective SiAlN coatings on pure Ti, Ti6Al4V, and Timetal 834 alloys in air at 800°C have been investigated and compared. After 50 h, the depleted SiAlN coating on Ti forms a  $\sim 5.0 \mu\text{m}$  thick oxide scale, and the SiAlN coating on Ti6Al4V is close to being depleted, while a 0.6  $\mu\text{m}$  thick remnant SiAlN coating without any oxidation has been observed on Timetal 834. The remnant SiAlN coating will not oxidise until it is close to being depleted or fully depleted. The depletion of SiAlN coatings induced by interfacial reaction with different substrates determined the degradation rates of the SiAlN coatings, which can be retarded by the presence of the non-reactive alloying elements Al and Sn in the Timetal 834 alloy or Ti6Al4V alloy. The degradation rate of protective SiAlN coating can be tailored by mitigating interfacial reaction via selecting a substrate with non-reactive alloying elements or building-up an interlayer with non-reactive alloy elements. Modifying the composition of the SiMeN coating ( $\text{Si}_3\text{N}_4/\text{MeN}$ , Me=Al, Zr, Ti, Cr, etc.), e.g. SiTiN, is also expected to reduce the interfacial reaction rate with underlying Ti or Ti alloy. Moreover, this innovative interface reaction control methodology can be potentially applied in other protective nitrides coating systems.

## Acknowledgment

PX would like to acknowledge support from Royal Academy of Engineering and Rolls-Royce for appointment of Rolls-Royce/Royal Academy of Engineering Research Chair in Advanced Coating Technology.

## Reference

- [1] A. Devaraj, V.V. Joshi, A. Srivastava, S. Manandhar, V. Moxson, V.A. Duz, C. Lavender, A low-cost hierarchical nanostructured beta-titanium alloy with high strength, *Nat. Commun.* 7 (2016) 11176.
- [2] M. Wang, Y. Lu, B. Pang, Z.T. Kloenne, H.L. Fraser, Y.L. Chiu, M.H. Loretto, Fine alpha in current and newly developed Ti alloys, *Acta Mater.* 173 (2019) 242-248.
- [3] L. Shao, G. Xie, X. Liu, Y. Wu, Q. Tan, L. Xie, S. Xin, F. Hao, J. Yu, W. Xue, K. Feng, Combustion behavior and mechanism of Ti-25V-15Cr compared to Ti-6Al-4V alloy, *Corros. Sci.* 194 (2022).
- [4] R. Liu, Y. Cui, L. Liu, B. Zhang, F. Wang, A primary study of the effect of hydrostatic pressure on stress corrosion cracking of Ti-6Al-4V alloy in 3.5% NaCl solution, *Corros. Sci.* 165 (2020).
- [5] D. Zhang, D. Qiu, M.A. Gibson, Y. Zheng, H.L. Fraser, D.H. StJohn, M.A. Easton, Additive manufacturing of ultrafine-grained high-strength titanium alloys, *Nature* 576(7785) (2019) 91-95.
- [6] J.A. Hooker, P.J. Doorbar, Metal matrix composites for aeroengines, *Mater. Sci. Technol.* 16(7-8) (2013) 725-731.
- [7] G. Chen, Y. Peng, G. Zheng, Z. Qi, M. Wang, H. Yu, C. Dong, C.T. Liu, Polysynthetic twinned TiAl single crystals for high-temperature applications, *Nat. Mater.* 15(8) (2016) 876-81.
- [8] J.C. Williams, E.A. Starke, Progress in structural materials for aerospace systems, *Acta Mater.* 51(19) (2003) 5775-5799.
- [9] W. Li, S. Zhu, C. Wang, M. Chen, M. Shen, F. Wang, SiO<sub>2</sub>-Al<sub>2</sub>O<sub>3</sub>-glass composite coating on Ti-6Al-4V alloy: Oxidation and interfacial reaction behavior, *Corros. Sci.* 74 (2013) 367-378.
- [10] Z. Gao, Z. Zhang, X. Zhang, J. Kulczyk-Malecka, H. Liu, P. Kelly, P.J. Withers, P. Xiao, A conformable high temperature nitride coating for Ti alloys, *Acta Mater.* 189 (2020) 274-283.
- [11] J. Musil, Hard nanocomposite coatings: Thermal stability, oxidation resistance and toughness, *Surf. Coat. Technol.* 207 (2012) 50-65.
- [12] P.H. Mayrhofer, C. Mitterer, L. Hultman, H. Clemens, Microstructural design of hard coatings, *Prog. Mater. Sci.* 51(8) (2006) 1032-1114.
- [13] W.W. Xu, S.L. Shang, B.C. Zhou, Y. Wang, L.J. Chen, C.P. Wang, X.J. Liu, Z.K. Liu, A first-principles study of the diffusion coefficients of alloying elements in dilute alpha-Ti alloys, *Phys. Chem. Chem. Phys.* 18(25) (2016) 16870-81.
- [14] J.-W. Lu, Y.-Q. Zhao, P. Ge, H.-Z. Niu, Microstructure and beta grain growth behavior of Ti-Mo alloys solution treated, *Mater. Charact.* 84 (2013) 105-111.

- [15] Y. Lu, J. Yang, W. Lu, R. Liu, G. Qiao, C. Bao, The mechanical properties of co-continuous Si<sub>3</sub>N<sub>4</sub>/Al composites manufactured by squeeze casting, *Mater. Sci. Eng. A* 527(23) (2010) 6289-6299.
- [16] J. Avila, J.L. Sacedón, Reactivity at the Al/Si<sub>3</sub>N<sub>4</sub> interfaces, *Appl. Phys. Lett.* 66(6) (1995) 757-759.
- [17] Z. Gao, J. Kulczyk-Malecka, Z. Zhang, H. Liu, X. Zhang, Y. Chen, P. Hill, P. Kelly, P. Xiao, Oxidation and degradation of amorphous SiAlN coating via forming Si-Si bond, *Corros. Sci.* 183 (2021).
- [18] J. Liu, C. Dong, X. Lu, Z. Qiao, F. Zhou, W. Liu, R. Riedel, Sn-containing Si<sub>3</sub>N<sub>4</sub>-based composites for adaptive excellent friction and wear in a wide temperature range, *J. Eur. Ceram. Soc.* 42(3) (2022) 913-920.
- [19] M.H.G. Jacobs, P.J. Spencer, A thermodynamic evaluation of the system Si-Sn, *Calphad* 20 (1996) 89-91.
- [20] Z. Gao, J. Kulczyk-Malecka, P. Kelly, P. Xiao, Effects of interfacial depletion on the degradation of SiAlN coating, *Appl. Surf. Sci.* 611 (2023) 155576.